Preprints.org

Article

Not peer-reviewed version

Carbonized Leather Waste with Deposited Polypyrrole Nanotubes: Conductivity and Dye Adsorption

Jaroslav Stejskal *, Fahanwi Asabuwa Ngwabebhoh, Miroslava Trchová, Jan Prokeš

Posted Date: 13 September 2023

doi: 10.20944/preprints202309.0810.v1

Keywords: bicontinuous composites; carbonized leather waste; conducting polymer; globular polypyrrole; polypyrrole nanotubes; conductivity; resistivity; dye adsorption; Raman spectra

Preprints.org is a free multidiscipline platform providing preprint service that is dedicated to making early versions of research outputs permanently available and citable. Preprints posted at Preprints.org appear in Web of Science, Crossref, Google Scholar, Scilit, Europe PMC.

Copyright: This is an open access article distributed under the Creative Commons Attribution License which permits unrestricted use, distribution, and reproduction in any medium, provided the original work is properly cited.

Preprints (www.preprints.org) | NOT PEER-REVIEWED | Posted: 13 September 2023 doi:10.20944/preprints202309.0810.v1

Disclaimer/Publisher's Note: The statements, opinions, and data contained in all publications are solely those of the individual author(s) and contributor(s) and not of MDPI and/or the editor(s). MDPI and/or the editor(s) disclaim responsibility for any injury to people or property resulting from any ideas, methods, instructions, or products referred to in the content.

Article

Carbonized Leather Waste with Deposited Polypyrrole Nanotubes: Conductivity and Dye Adsorption

Jaroslav Stejskal [1,*], Fahanwi Asabuwa Ngwabebhoh [1], Miroslava Trchová [2] and Jan Prokeš [3]

[1] University Institute, Tomas Bata University in Zlin, 760 01 Zlin, Czech Republic
[2] Central Laboratories, University of Chemistry and Technology, Prague, 166 28 Prague 6, Czech Republic
[3] Faculty of Mathematics and Physics, Charles University, 180 00 Prague 8, Czech Republic
* Correspondence: stejskal@utb.cz

Abstract: Leather waste was carbonized at 800 °C in inert atmosphere. The resulting biochar was coated in situ with polypyrrole nanotubes produced by the oxidation of pyrrole in the presence of methyl orange. The composites of carbonized leather with deposited polypyrrole nanotubes of various composition were compared with similar composites based on globular polypyrrole. Their molecular structure was characterized by infrared and Raman spectra. Both conducting components formed a bicontinuous structure. The resistivity determined by four-point van der Pauw method was monitored as a function of pressure applied up to 10 MPa. The typical conductivity of composites was of the order of tenths to units S cm^{-1} and it was always higher for polypyrrole nanotubes than for globular polypyrrole. The conductivity decreased by 1–2 orders of magnitude after treatment with ammonia but still maintained a level acceptable for applications operating under non-acidic conditions. The composites were tested for dye adsorption, viz. cationic methylene blue and anionic methyl orange, using UV-spectroscopy. The composites are designed for the future use as functional adsorbents controlled by the electrical potential.

Keywords: bicontinuous composites; carbonized leather waste; conducting polymer; globular polypyrrole; polypyrrole nanotubes; conductivity; resistivity; dye adsorption; Raman spectra

1. Introduction

Novel functional materials are often based on the design of nanostructured composites, which display attractive properties and can be applied in new directions. The present study aims at the preparation of conducting materials comprising organic nitrogen-containing carbon obtained by the carbonization of leather waste and conducting polymer, polypyrrole, with special attention paid to its nanotubular form. Both components are conducting at semiconductor level and, while the former component is a product of environmental friendly process, the latter is a representative of responsive redox-active polymers. The fibrous biochar obtained from leather with conducting polymer deposited at its surface results in bicontinuous structure that is favourable for the conduction [1].

Bicontinuous composites composed of two interpenetrating phases have often been reported in the literature and concern typically inorganic systems. They display improved mechanical and electrical properties compared with simple mixtures of components. The term of three-dimensional interpenetrating matrices of two different phases [2] has been used specially for inorganic combinations of ceramics, e.g., alumina/titanium aluminide [3] or ceramics combined with metals, e.g., silicon carbide/aluminium [4] or silica/aluminium [5]. Inorganic and organic components have also been combined and are represented by either fibrous inorganic component dispersed in organic polymer matrix, e.g., silver nanowire network in polyurethane matrix [6] or, vice versa, by porous inorganics filled with organic polymers, e.g., alumina penetrated with polycarbonate [7].

In the organic realm, bicontinuous composites should be distinguished from interpenetrating polymer networks where the three-dimensional structure is based on individual polymer chains and not by the phases composed of multiple polymer threads in the composites. From organic composites, melamine sponge coated with conducting polymers [8], or fibrous collagen structure of leather modified in a similar manner may serve as examples [9].

© 2023 by the author(s). Distributed under a Creative Commons CC BY license.

Preprints (www.preprints.org) | NOT PEER-REVIEWED | Posted: 13 September 2023 doi:10.20944/preprints202309.0810.v1

Carbonization of leather waste to a fibrous conducting nitrogen-containing biochar, i.e., a waste to useful material, has been reported [10–12]. Applications involving this type of biochar concern dye adsorbents [13,14], removal of harmful chromium(VI) from wastewater [15,16], electromagnetic radiation shielding [11], supercapacitor electrodes [17,18], batteries [19,20] or fuels [21,22]. In some of them electrical conduction is required in others it is of potential benefit.

The carbons derived from leather waste are produced as macroporous sponges with poor mechanical properties and as intractable powder after they were pulverized. They can be directly used as fillers in construction materials [23,24]. On the other hand they can be converted to functional nanomaterials by coating with conducting, polymers, such as polyaniline [1] or polypyrrole, as demonstrated in present study. Such composites could be compressed to solid materials with applicable mechanical integrity and may benefit from the similar or complementary properties of both components (Table 1).

Table 1. Properties of composite components, carbonized leather and polypyrrole.

Property	Carbonized leather	Polypyrrole
Conductivity	10^{-8}–10^{0} S cm^{-1}	10^{-1}–10^{1} S cm^{-1}
pH Sensitivity of conductivity	none	reduced above pH 4–6
Thermal stability	stable	converts to carbon
Molecular structure	carbonaceous, graphitic	conjugated polymer chains
Supramolecular structure	fibrous	globules or nanotubes
Specific surface area	activation dependent	low
Redox activity	none	yes
Dye adsorption	yes	yes

The present manuscript reports mainly electrical properties of polypyrrole composites with carbonized leather and illustrates their application for dye removal in the water-pollution treatment. Although such use is not associated directly with conductivity, the adsorption control by the applied electrical potential is a route to the functional adsorbents.

2. Experimental

2.1. Preparation

Chrome-plated pigskin leather with 0.8 mm average thickness was provided by the Footwear Research Centre, Tomas Bata University in Zlin, Czech Republic, and used for the simulation of the waste. Pyrrole, iron(III) chloride hexahydrate, hydrochloric acid, ethanol, ammonium hydroxide, methylene blue and methyl orange dyes were supplied (Sigma Aldrich, Prague, Czech Republic) and used as delivered.

Leather was shredded into fibers and carbonized in a horizontal tubular vacuum furnace GSL-1600X (Carbolite Gero, Neuhausen, Germany). The temperature increased at 5 °C min^{-1} rate to 800 °C under 50 mL min^{-1} argon flow. After 1 h, the power was switched off, the product was left to cool still under inert atmosphere and homogenized using a ball mill. The product contained 70.7 wt% carbon, 7.6 wt% nitrogen and 12.6 wt% chromium [25].

Polypyrrole coating was deposited in situ during the polymerization of pyrrole (Figure 1). Parts of the carbonized leather were dispersed in 0.2 M aqueous pyrrole solution under stirring at room temperature. The same volume of 0.5 M iron(III) chloride solution was added. The reaction mixture thus contained 0.1 M pyrrole and 0.25 M iron(III) chloride. Based on stoichiometry (Figure 1), 100 mL of mixture is expected to produce about 1 g of globular polypyrrole but the true yield may be somewhat affected by the type and number of counter-ions. The volumes of reactant solutions were varied to obtain *ca* 1 gram of composites (Table 2). Polypyrrole nanotubes were deposited in similar manner, only reaction mixture contained in addition 0.005 M methyl orange. The dye was dissolved along with pyrrole. After 1 h allowed for the pyrrole polymerization, dark precipitates were collected

Preprints (www.preprints.org) | NOT PEER-REVIEWED | Posted: 13 September 2023 doi:10.20944/preprints202309.0810.v1

on a filter, well rinsed with 0.2 M hydrochloric acid, then with ethanol, and left to dry in air. A part of the some samples was deprotonated by overnight suspension in 1M ammonium hydroxide.

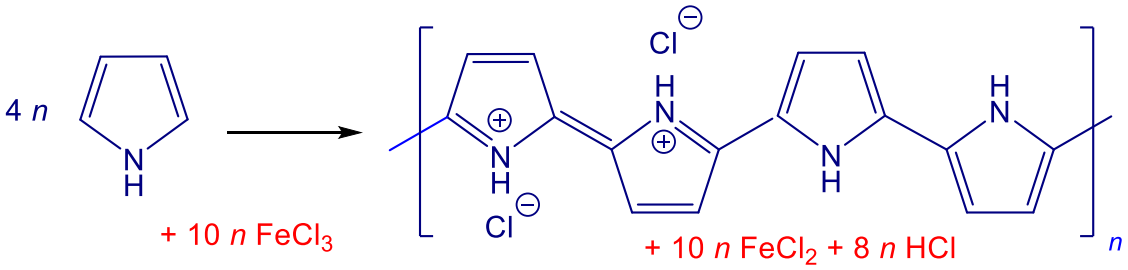

Figure 1. The oxidation of pyrrole with iron(III) chloride yields polypyrrole hydrochloride.

Table 2. The protocol for the preparation of *ca* 1 g of composites composed of polypyrrole (PPy) and carbonized leather with gradually increasing polypyrrole content, and the experimental yield.

Composition, wt% PPy	Carbonized leather, g	+0.2 M Pyrrole, mL	+0.25 M $FeCl_3$, mL	PPy, g	Yield, g
20	0.8	10	10	0.2	1.041
40	0.6	20	20	0.4	1.102
50	0.5	25	25	0.5	1.181
60	0.4	30	30	0.6	1.266
80	0.2	40	40	0.8	1.351
100	0	50	50	1	1.543

2.2. Morphology

Scanning electron microscopy was performed using a Nova NanoSEM electron microscope (FEI, Brno, Czech Republic) to reveal the morphology of polypyrrole and its composite with carbonized leather. Prior to analysis, the materials were gold sputter-coated using a JEOL JFC 1300 Auto Fine coater (JEOL, Tokyo, Japan).

2.3. Spectroscopy

FTIR spectra were collected with a Nicolet 6700 spectrometer (Thermo Fisher Scientific, Waltham, MA, USA) using a reflective ATR extension GladiATR (PIKE Technologies, Fitchburg, WI, USA). Spectra were recorded in the 4000–400 cm^{-1} range at 4 cm^{-1} resolution, 64 scans and Happ-Genzel apodization. Raman spectra were recorded with a Thermo Scientific DXR Raman microscope (Thermo Fisher Scientific, Waltham, MA, USA) operating with a 780 nm laser line. The laser beam was focused by 50× objective. The scattered light was analysed by a spectrograph with holographic gratings 900 lines mm^{-1} and a 50 μm pinhole width. The acquisition time was 10 s with 10 repetitions.

2.4. Electrical properties

The resistivity was determined by a four-point van der Pauw method using a lab-made press based on a cylindrical glass cell with an inner diameter of 10 mm [8]. The powders were placed between glass support and a glass piston carrying four platinum/rhodium wire electrodes at its perimeter. The set-up used a current source a Keithley 220, a Keithley 2010 multimeter and a Keithley 705 scanner with a Keithley 7052 matrix card (Keithley Instruments Inc., Cleveland, OH, USA). The pressure up to 10 MPa (=102 kg cm^{-2}) was recorded with a L6E3 strain gauge cell (Zemic Europe BV, Etten-Leur, The Netherlands). The force was applied with an E87H4-B05 stepper motor (Haydon Switch & Instrument Inc., Waterbury, CT, USA). The sample thickness was monitored during the compression by a dial indicator Mitutoyo ID-S112X (Mitutoyo Corp., Sakado, Japan). The resistivity

Preprints (www.preprints.org) | NOT PEER-REVIEWED | Posted: 13 September 2023 doi:10.20944/preprints202309.0810.v1

was also measured on composite pellets prepared after compression at 527 MPa by a manual hydraulic press (Specac, Orpington, UK).

2.5. Dye Adsorption

The performance of composites in the removal of anionic and cationic dyes from aqueous solutions was studied with UV-vis spectroscopy. The dye adsorption was followed in a batch reactor for 24 h at 25 °C, pH 5.5, initial dye concentration 100 mg L^{-1}, and sample dosage 500 mg L^{-1}. The adsorption was monitored by recording optical absorption with a Varian Cary 100 UV-Vis spectrophotometer (Varian Inc., Palo Alto, CA, USA) in a 0.2 cm cell at absorption maxima 466 and 594 nm for methyl orange and methylene blue, respectively. The dye removal efficiency was then calculated as $R(\%) = (A_0 - A_e)/A_0 \times 100$ [26], where A_0 and A_e were optical absorptions at start and in equilibrium, respectively.

3. Results and Discussion

3.1. Preparation

Polypyrrole is prepared by the oxidation of pyrrole in aqueous medium, iron(III) chloride being the most popular oxidant [27] (Figure 1). The product has a characteristic globular morphology (Figure 2). It has been well established by transmission electron microscopy that polypyrrole nanotubes are produced instead when the polymerization is carried out in the presence methyl orange [28,29]. The change in morphology is associated with the increase in conductivity by about one order of magnitude. Other organic dyes are also able to affect the morphology and conductivity of polypyrrole [30] but methyl orange performs the best.

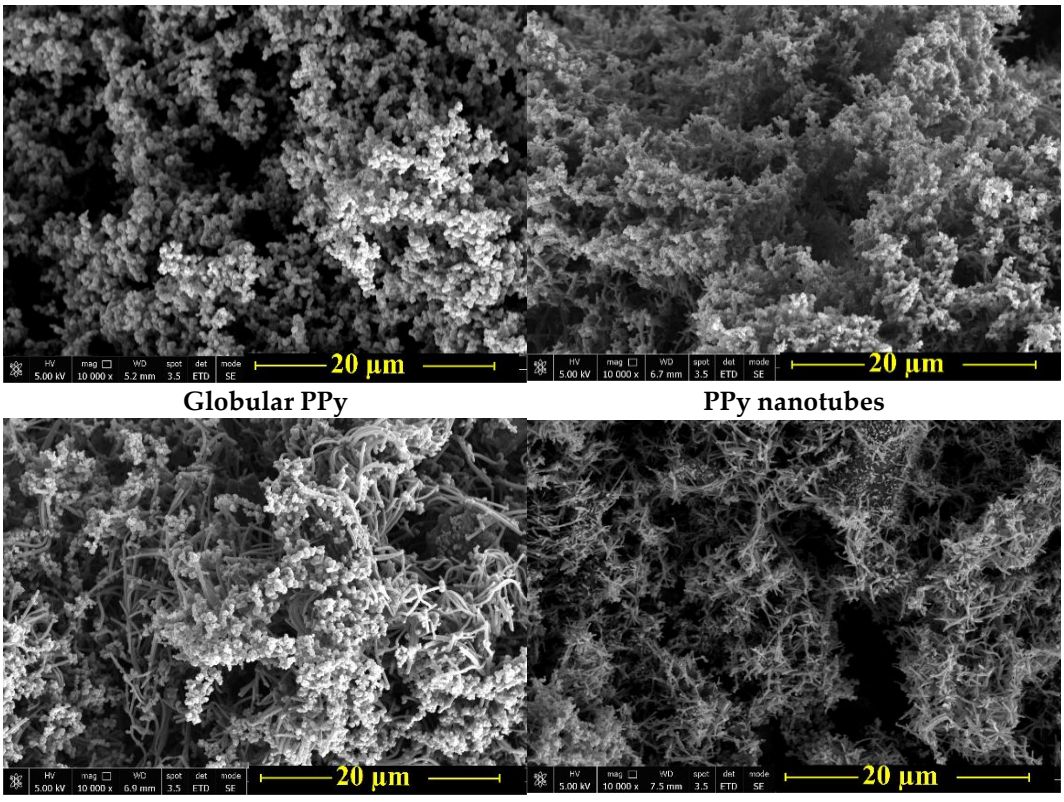

Figure 2. SEM micrographs of globular polypyrrole (top left) and polypyrrole nanotubes (top right) and their composites after the deposition of polypyrrole on carbonized leather (bottom).

Any substrate immersed in the reaction medium used for the preparation of polypyrrole or polyaniline becomes coated with a thin film of this polymer and polymer nanoparticles adhere to its

Preprints (www.preprints.org) | NOT PEER-REVIEWED | Posted: 13 September 2023 doi:10.20944/preprints202309.0810.v1

surface [8,9,31–33]. When it comes to the resulting composites, the composite morphology becomes more complex (Figure 2). In the absence of methyl orange, polypyrrole globules adhere on the polypyrrole-coated carbonized collagenous fibres constituting the original leather. The morphology becomes more uniform, when in the presence of methyl orange well-developed polypyrrole nanotubes completely coat the carbonized leather fibres.

3.2. Spectroscopy

FTIR spectra of polypyrrole do not depend on the polypyrrole morphology and only the spectra of composites with polypyrrole nanotubes are demonstrated (Figure 3). The infrared spectrum of carbonized leather is practically featureless. After coating with polypyrrole nanotubes we observe the main bands of polypyrrole due to the surface sensitive nature of the ATR spectroscopic technique with the penetration depth of a few micrometres of infrared radiation. They are situated at 1528 cm^{-1} (C–C stretching vibrations in the pyrrole ring), 1447 cm^{-1} (C–N stretching vibrations in the ring), 1288 cm^{-1} (C–H or C–N in-plane deformation modes), 1143 cm^{-1} (breathing vibrations of the pyrrole rings), 1032 cm^{-1} (C–H and N–H in-plane deformation vibrations), and 958 cm^{-1} (C–H out-of-plane deformation vibrations of the ring) [29,34].

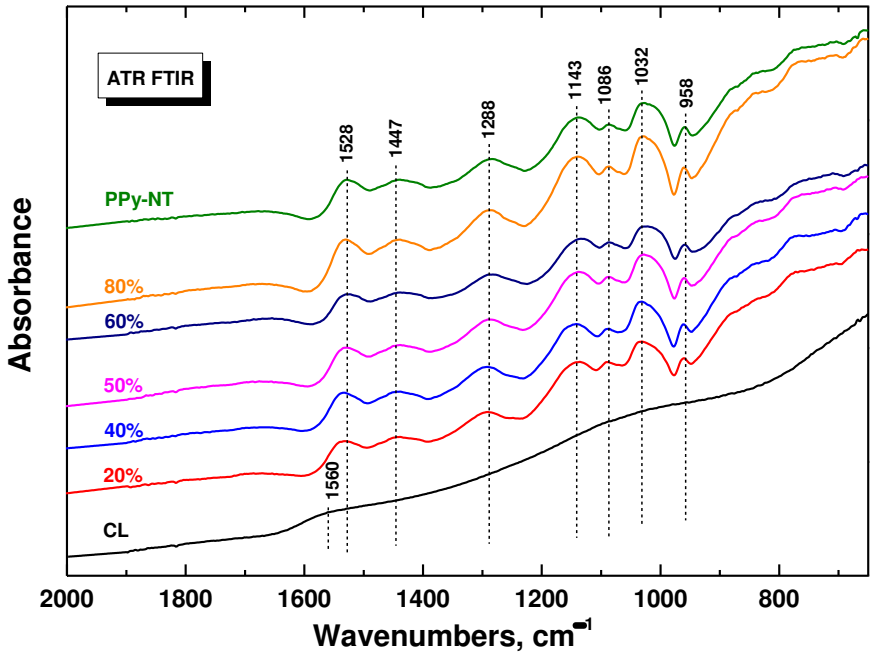

Figure 3. ATR FTIR spectra of carbonized leather (CL) coated with various amount of polypyrrole nanotubes (PPy-NT).

In the Raman spectrum of carbonized leather we detect the two main bands with local maxima at 1597 and 1323 cm^{-1} characteristic of carbon-like material [35] (Figure 4). After coating with polypyrrole nanotubes we observe, due to the resonance of the energy of the laser excitation wavelength 780 nm with the energy of polarons in the polypyrrole salt, mainly the bands of polypyrrole. This also confirms the complete coating of biochar with polypyrrole. The bands are situated at 1597 cm^{-1} and 1586 cm^{-1} (C=C stretching vibrations of polypyrrole backbone), 1391 and 1323 cm^{-1} (two bands of ring-stretching vibrations, the intensity of the latter increases after deprotonation), 1234 cm^{-1} (antisymmetric C–H deformation vibrations). The double peak with local maxima at 1082 and 1042 cm^{-1} corresponds to C–H out-of-plane deformation vibrations, the second becomes sharper after deprotonation). The band at 968 cm^{-1} of the ring-deformation vibrations in

Preprints (www.preprints.org) | NOT PEER-REVIEWED | Posted: 13 September 2023 doi:10.20944/preprints202309.0810.v1

neutral polypyrrole units and the sharp peak at 922 cm^{-1} of the ring-deformation vibrations in dication (bipolaron) units are also detected in the spectra [29].

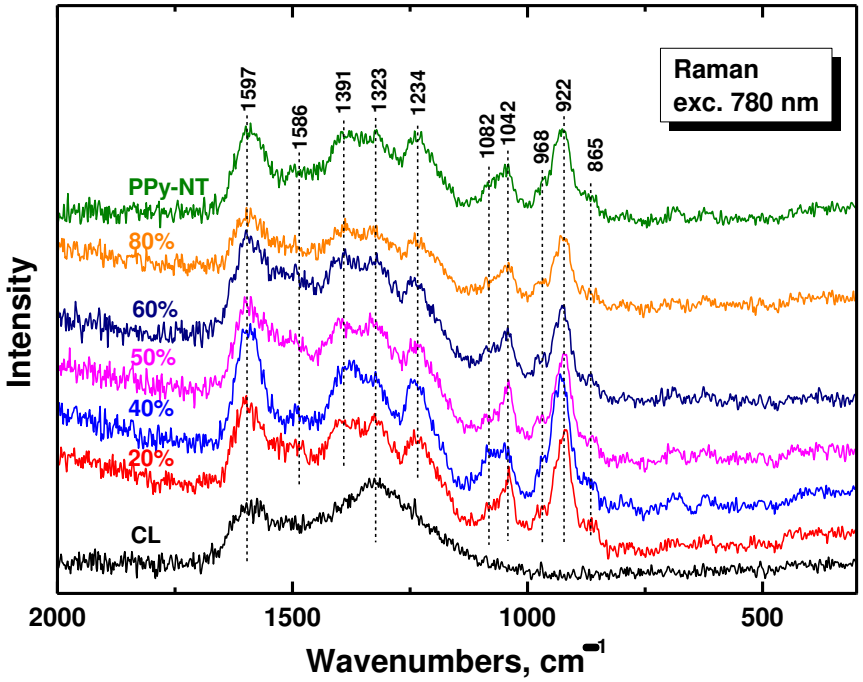

Figure 4. Raman spectra of carbonized leather (CL) coated with various amounts of polypyrrole nanotubes (PPy-NT).

3.3. Electrical Properties

Both composite components are conducting at semiconductor level (Table 1). Some materials cannot be compressed to pellets used for the routine determination of resistivity. For that reason, the resistivity has to be determined on powder compressed under defined pressure. This quantity thus becomes pressure-dependent and the resistivity decreases during compression [36,37]. The present study thus uses a four-point method [8], which is preferred to the two-point procedure because of the relatively high conductivity of samples.

Carbonized leather has the resistivity of the same order of magnitude as globular polypyrrole [12], and the same applies for their composites (Figure 5a). The analogous samples with polypyrrole nanotubes are more conducting, their resistivity being lower by *ca* one order of magnitude (Figure 5b). The pressure dependences of resistivity are linear in double-logarithmic presentation in both cases, and for all composites they have a similar slope. The dependence for neat carbonized leather is steeper and this in the accordance with different mechanical properties (cf. below).

Preprints (www.preprints.org) | NOT PEER-REVIEWED | Posted: 13 September 2023 doi:10.20944/preprints202309.0810.v1

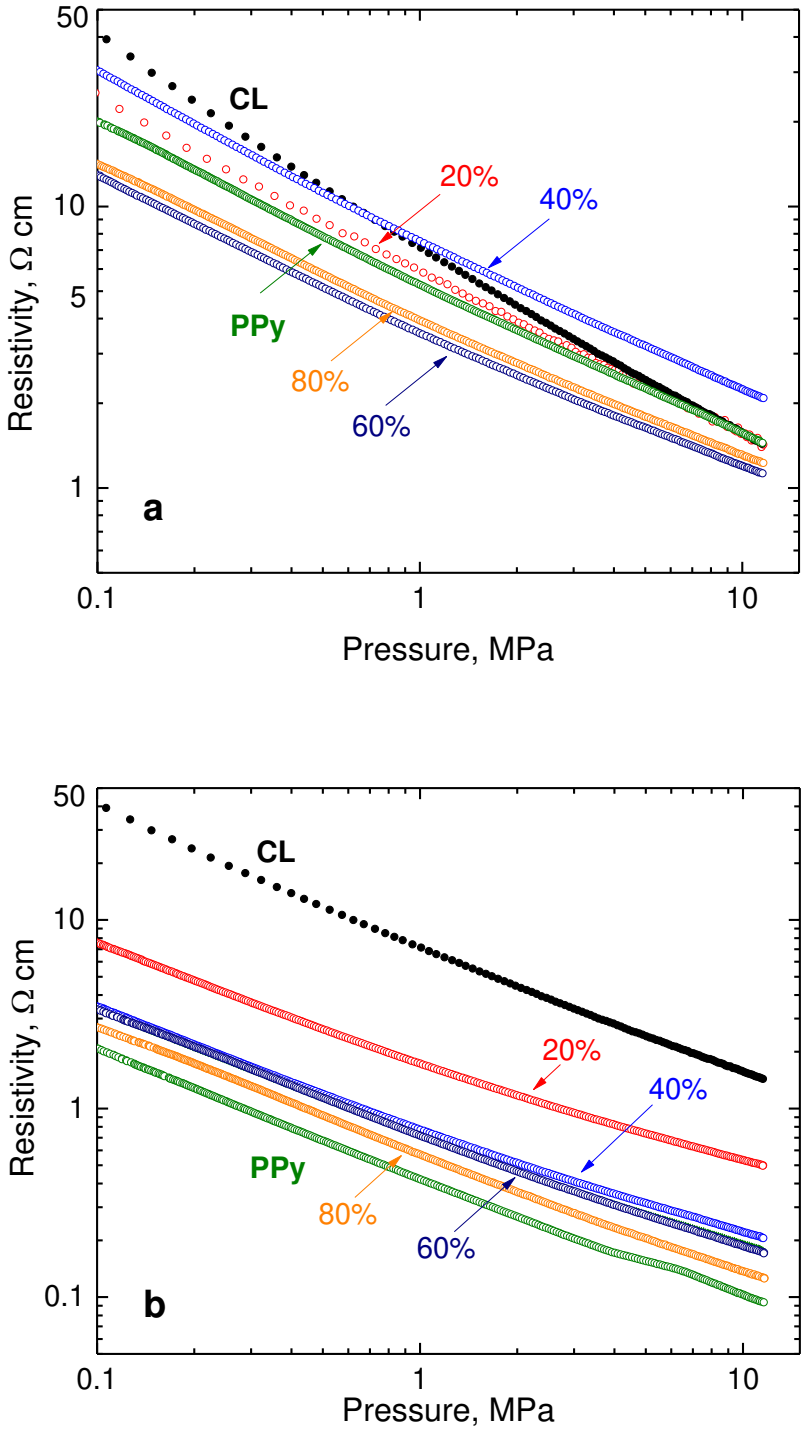

Figure 5. The pressure dependence of the resistivity of leather carbonized at 800 °C (CL) coated with various amount of (a) globular polypyrrole (PPy-G) and (b) polypyrrole nanotubes (PPy-NT).

The resistivity of the individual samples at 1 and 10 MPa pressures are available in Figure 6, and they provide the rather trivial information that (1) the resistivity only little varies with the composition, (2) it becomes lower at higher pressure, and (3) composites with polypyrrole nanotubes have significantly lower resistivity compared to those with globular polypyrrole. For the readers preferring the presentation in terms of conductivity rather than the reciprocal resistivity, some key values are provided in Table 3.

Preprints (www.preprints.org) | NOT PEER-REVIEWED | Posted: 13 September 2023 doi:10.20944/preprints202309.0810.v1

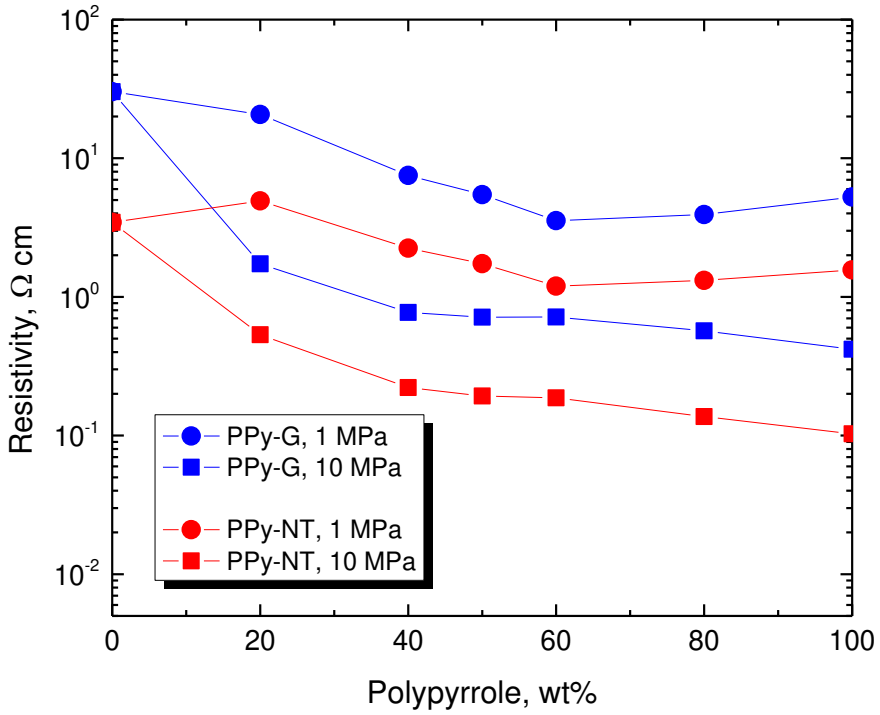

Figure 6. Resistivity of composites of globular polypyrrole or polypyrrole nanotubes and carbonized leather compressed at 1 MPa and 10 MPa.

Table 3. Conductivity (S cm^{-1}) of leather carbonised at 800 °C (CL), globular polypyrrole (PPy-G) or polypyrrole nanotubes (PPy-NT) and their composites (50 wt%) determined at 1 or 10 MPa pressure or with free-standing compressed pellet (527 MPa).

Sample	1 MPa	10 MPa	Pellet
CL	0.269	3.71	(a)
PPy-G	0.190	0.637	2.55
PPy-NT	2.38	9.71	38.6
PPy-G/CL	0.183	0.575	1.96
PPy-NT/CL	1.40	5.18	16.1

[a] A pellet could not be prepared.

3.4. Mechanical Properties

The experimental setup used for the determination of resistivity allows also to follow the sample thickness during the compression [8], i.e., to assess also some features of mechanical behaviour. They were similar for both types of polypyrrole and only the results concerning the deposition of polypyrrole nanotubes are reported (Figure 7). The double-logarithmic dependences of sample thickness on pressure are close to linear for all composites. The steeper the dependences are, the fluffier are the composites and easier they are compressed. The absolute values of slopes decrease only slowly as the content of polypyrrole increases. The carbonized leather alone is the most difficult to compress and resembles inorganic rather than organic materials.

Preprints (www.preprints.org) | NOT PEER-REVIEWED | Posted: 13 September 2023 doi:10.20944/preprints202309.0810.v1

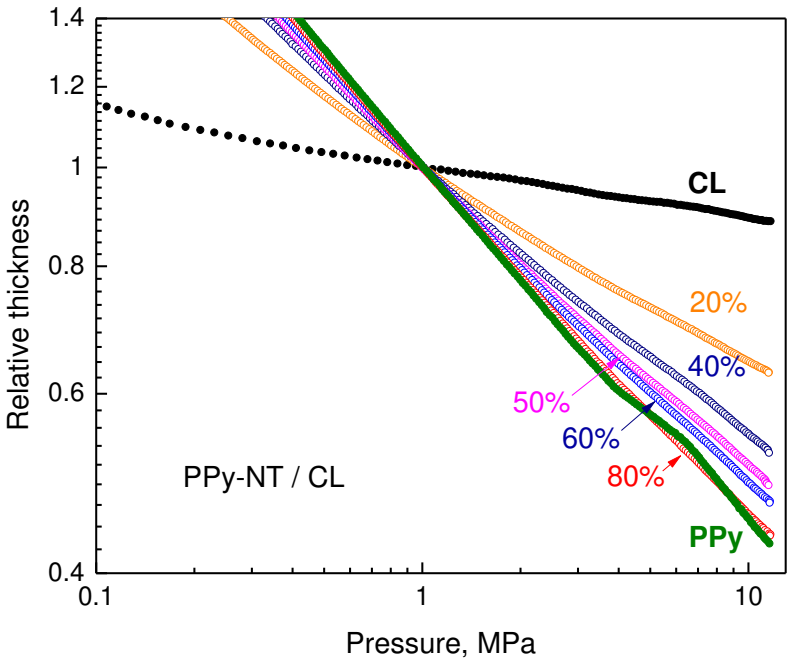

Figure 7. The change of sample thickness during the compression normalized to the thickness at 1 MPa.

3.5. Deprotonation

For some applications, e.g., in biomedicine, the effect of pH may become of importance. The conductivity of carbonized leather is not affected by pH [1]. The conductivity of polypyrrole, however, becomes reduced by several orders of magnitude in alkaline ammonia solution due to the deprotonation of polypyrrole salt (Figure 1) to less conducting base [38] but the polymer still retains most of its conductivity. The similar behaviour applies to the composite with carbonized leather. For example, the conductivity of polypyrrole nanotubes (50 wt%)/carbonized leather was reduced after treatment with ammonia solution by about two orders of magnitude (Figure 8), viz. from 16.1 S cm^{-1} to 0.0195 S cm^{-1} when measured on compressed pellet, i.e., a good level of conductivity was maintained regardless of non-acidic pH treatment.

Preprints (www.preprints.org) | NOT PEER-REVIEWED | Posted: 13 September 2023 doi:10.20944/preprints202309.0810.v1

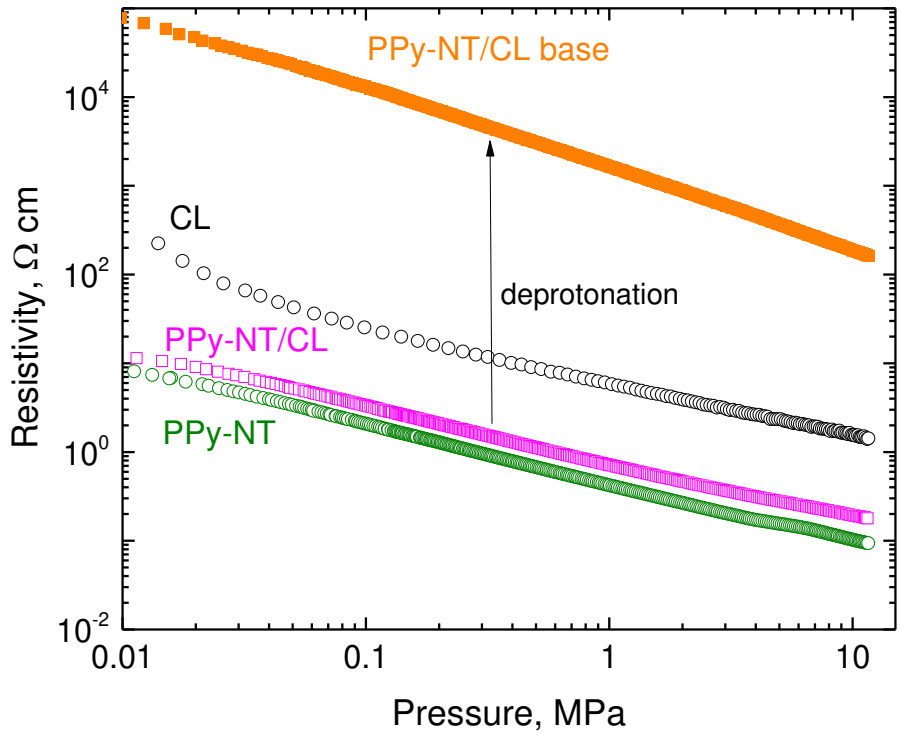

Figure 8. The pressure dependences of resistivity of polypyrrole nanotubes (PPy-NT) and their composites (50 wt% PPy) with carbonized leather and the effect of composite deprotonation.

3.6. Dye Adsorption

One of the application area is shared by microstructured carbons and conducting polymers – the adsorption of water pollutants. The removal of organic dyes from wastewater is based on the adsorption and/or the photocatalytic decomposition by reactive oxygen species [39–41] or by the biodegradation [42,43]. Electrocatalytic dye destruction employing conducting polymers is also possible [44,45]. There are two reasons for introducing polypyrrole to hybrid composites used as adsorbents: (1) Conducting polymers and dyes share features of molecular structure, i.e., the presence of nitrogen atoms and aromatic rings. In addition to dispersion forces, nitrogen atoms participate in hydrogen bonding and the benzene rings allow for the attractive π–π interactions supporting the adsorption. Electrostatic interactions between polypyrrole polycation (Figure 1) and anionic dyes may also be operational. (2) In the contrast to carbonaceous adsorbents, conducting polymers are electroactive and responsive, i.e., the respond to external stimuli by the change in electrical properties. Molecular structure of conducting polymers can be switched between protonated salt and base forms, as well as oxidized and reduced structures in the response to applied pH or electrical potential, respectively [46,47].

The feasibility of dye removal has been tested in present study with cationic methylene blue and anionic methyl orange dyes (Figure 9). The results are only an illustration of feasibility and experiments have not been optimized with respect to dye and composite concentrations or other parameters. While the dye adsorption at original leather was marginal, it improved for both dyes after carbonization. The adsorption of methylene blue was lower compared with methyl orange and it slowly decreased with increasing content of polypyrrole in the composites. On the other hand, the adsorption of methyl orange had increasing trend as may be expected for an anionic dye at polypyrrole polycation. The similar adsorption performance has been found regardless of polypyrrole morphology (Figure 9).

Preprints (www.preprints.org) | NOT PEER-REVIEWED | Posted: 13 September 2023 doi:10.20944/preprints202309.0810.v1

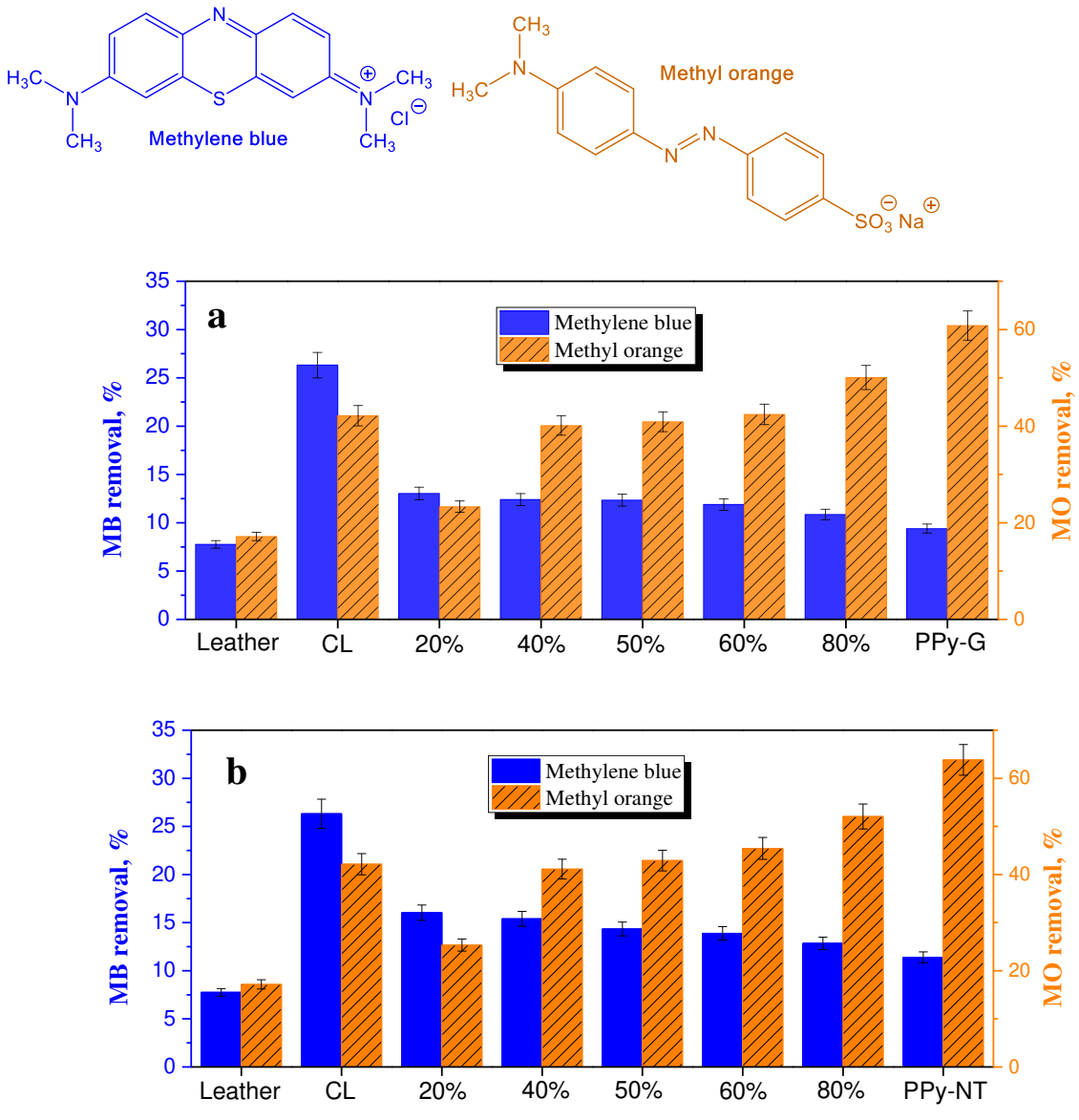

Figure 9. Removal of dyes, methylene blue and methyl orange, with leather, carbonized leather and composites of carbonized leather with different percentage of polypyrrole (a) globules and (b) nanotubes. N.B. The scales for both dyes are different.

4. Conclusions

The carbonized leather waste was coated with polypyrrole during the polymerization of pyrrole. The resistivity of resulting composite powders decreased during the compression up to 10 MPa. The conductivity of composites was little dependent on the polypyrrole content in composites and was of the order of tenths S cm^{-1} for globular polypyrrole and units S cm^{-1} for polypyrrole nanotubes at 10 MPa. The conductivity of composites compressed to pellets was still about one order of magnitude higher. The conductivity decreased by *ca* two orders of magnitude after deprotonation of polypyrrole with ammonia but maintained a level acceptable for applications operating under alkaline or close to neutral physiological conditions. When tested for dye adsorption, the composites rich in carbonized leather adsorbed better a cationic dye, methylene blue, while those containing more polypyrrole preferentially removed anionic dye, methyl orange, from aqueous media regardless of polypyrrole morphology. While most of the properties of composites based on globular and nanotubular polypyrrole are comparable, due to the higher conductivity those with polypyrrole nanotubes are the

Preprints (www.preprints.org) | NOT PEER-REVIEWED | Posted: 13 September 2023 doi:10.20944/preprints202309.0810.v1

most prospective. The composites might be suitable for the further studies of dyes adsorption influenced or controlled by the applied electrical potential.

ORCID:
Jaroslav Stejskal – 0000-0001-9350-9647
Fahanwi Asabuwa Ngwabebhoh – 0000-0002-1492-1869
Miroslava Trchová – 0000-0001-6105-7578
Jan Prokeš – 0000-0002-8635-7056

Author Contributions: Jaroslav Stejskal: Conceptualization, Writing – Original Draft. Fahanwi Asabuwa Ngwabebhoh: Investigation, Formal Analysis. Miroslava Trchová: Methodology, Investigation. Jan Prokeš: Methodology, Data Curation.

Funding: The authors thank the Ministry of Education, Youth, and Sports of the Czech Republic (RP/CPS/2022/005) for financial support.

Conflict of Interest: The authors declare no conflict of interest.

References

1. Stejskal, J; Ngwabebhoh, A; Sáha, T; Prokeš, J. Coating of carbonized leather waste with the conducting polymer polyaniline: Bicontinuous composites for dye adsorption. Coatings 2023, 13, 1419. doi: 10.3390/coatings13081419
2. Binner, J; Chang, H; Higginson, R. Processing of ceramic–metal interpenetrating composites. J. Eur. Ceramic Soc. 2009, 9, 837–842. doi: 10.1016/j.jeurceramsoc.2008.07.034
3. Travitzky, N; Gotman, I; Claussen, N. Alumina-Ti aluminide interpenetrating composites: microstructure and mechanical properties. Mater. Lett. 2013, 57, 3422–3426. doi: 10.1016/S0167-577X(03)00090-9
4. Li, S; Li, YF; Wang, QW; Miao, K; Liang, X; Lu, ZL; Li, DC. Fabrication of 3D-SiC/aluminum alloy interpenetrating composites by DIW and pressureless infiltration. Ceram. Int. 2021, 47, 24340–24347. doi: 10.1016/j.ceramint.2021.05.147
5. Khan, SM; Deng, ZF; Yang, T; Li, L. Bio-inspired ceramic-metal composites using ceramic 3D printing and centrifugal infiltration. Adv. Eng. Mater. 2022, 24, 2101009. doi: 10.1002/adem.202101009
6. Hu, WL; Niu, XF; Zhao, R; Pei, QB. Elastomeric transparent capacitive sensors based on an interpenetrating composite of silver nanowires and polyurethane. Appl. Phys. Lett. 2013, 102, 083303. doi: 10.1063/1.4794143
7. Al-Jawoosh, S; Ireland, A; Su, B. Characterisation of mechanical and surface properties of novel biomimetic interpenetrating alumina-polycarbonate composite materials. Dental Mater. 2020, 36, 1595–1607. doi: 10.1016/j.dental.2020.09.016
8. Stejskal J; Vilčáková J; Jurča M; Fei HJ; Trchová M; Kolská Z; Prokeš J; Křivka I. Polypyrrole-coated melamine sponge as a precursor for conducting macroporous nitrogen nitrogen-containing carbons. Coatings 2022, 12, 324. doi: 10.3390/coatings12030324
9. Ngwabebhoh, FA; Zandraa, O.; Sáha, T; Stejskal, J; Trchová, M; Kopecký, D; Pfleger, J; Prokeš, J. *In-situ* coating of leather with conducting polyaniline in colloidal dispersion mode. Synth. Met. 2022, 291, 117191. doi: 10.1016/j.synthmet.2022.117191
10. Yılmaz, O; Kantarli, I; Yuksel, M; Saglam, M; Yanik, J. Conversion of leather wastes to useful products. Resources Conserv. Recycling 2007, 49, 436–448. doi: 10.1016/j.resconrec.2006.05.006
11. Yuan, B; Lai, SX; Li, JJ; Li, L; Bai, SB. Trash into treasure: stiff, thermally insulating and highly conductive carbon aerogels from leather wastes for high-performance electromagnetic interference shielding. J. Mater. Chem. C 2021, 9, 2209–2310. doi: 10.1039/d0tc05480a
12. Stejskal, J; Ngwabebhoh, FA; Sáha, P; Prokeš, J. Carbonized leather waste: A review and conductivity outlook. Polymers 2023, 15, 1028. doi: 10.3390/polymers 15041028
13. Foo, KY; Hameed, BH. An overview of dye removal via activate carbon adsorption proces. Desalin. Water. Treat. 2010, 19, 255–274. doi: 10.5004/dwt.2010.1214
14. Gupta, R; Pandit, C; Pandit, S; Gupta, PK; Lahiri, D; Agarwal, D; Pandey, S. Potential and future prospects of biochar-based materials and their applications in removal of organic contaminants from industrial wastewater. J. Mater. Cycles Waste Management 2022, 24, 852–876. doi: 10.1007/s10163-022-01391-z
15. Bashir, MA; Khalid, M; Naveed, M; Ahmad, R; Gao, B. Influence of feedstock and pyrolytic temperature of biochar on physico-chemical characteristics and sorption of chromium in tannery polluted soil. Int. J. Agricult. Biol. 2018, 20, 2823–2834. doi: 10.17957/IJAB/15.0841
16. Sun, XG; Peng, QF; Wang, ZX; Li, CM; Huang, YQ. N-doped porous carbon derived from Cr-tanned leather shaving wastes for synergetic adsorption of Cr(VI) from aqueous solution. Mater. Lett. 2021, 284, 128815. doi: 10.1016/j.matlet.2020.128815
17. Ma, F; Ding, SL; Ren, HJ; Peng, PL. Preparation of chrome-tanned leather shaving-based hierarchical porous carbon and its capacitance properties. RSC Adv. 2019, 9, 18333–18343. doi: 10.1039/c9ra03139a

Preprints (www.preprints.org) | NOT PEER-REVIEWED | Posted: 13 September 2023 doi:10.20944/preprints202309.0810.v1

18. Liu, PY; Xing, ZH; Wang, X; Diao, S; Duan, BR; Yang, C; Shi, L. Nanoarchitectonics of nitrogen-doped porous carbon derived from leather wastes for solid-state supercapacitor. J. Mater. Sci., Mater. Electron. 2022, 33, 4887–4901. doi: 10.1007/s10854-021-07678-5
19. Ashokkumar, M; Narayanan, NT; Reddy, ALM; Gupta, BK; Chandrasekaran, B; Talapatra, S; Ajayan, PM; Thanikaivelan, P. Transforming collagen wastes into doped nanocarbons for sustainable energy applications. Green Chem. 14 (2012) 1689–1695. doi: 10.1039/c2gc35262a
20. Han, WY; Wang, HL Xia, KD; Chen, SS; Yan, PX; Deng, TS; Zhu, WB. Superior nitrogen-doped activated carbon materials for water cleaning and energy storing prepared from renewable leather wastes. Environ. Int. 142 (2020) 105846. doi: 10.1016/j.envint.2020.105846
21. Torres, A; Lange, LC; de Melo, GCB; Praes, GE. Pyrolysis of chromium rich tanning industrial wastes and utilization of carbonized wastes in metallurgical process. Waste Management 2016, 48, 448–456. doi: 10.1016/j.wasman.2015.11.046
22. Shi, AR; Song, XM; Wei, L; Ma, HY; Pang, HJ; Li, WW; Liu, XW; Tan, LC. Design of an internal/external bicontinuous conductive network for high-performance asymmetrical supercapacitors. Molecules 2023, 27, 8168. doi: 10.3390/molecules27238168
23. Murugan, KP; Swarnalatha, S; Sekaran, G. Chromium impregnated carbon fibres from tannery buffing dust waste for road applications. Mater. Today, Proc. 2016, 3, 3703–3708. doi: 10.1016/j.matpr.2016.11.016
24. Enfrin, M; Giustozzi, F. Recent advances in the construction of sustainable asphalt roads with recycled plastic. Polym. Int. 2022, 71, 1316–1383. doi: 10.1002/pi.6405
25. Grycová, B; Klemencová, K; Leštinský, P; Stejskal, J; Sáha, T.; Trchová, M; Prokeš, J. Conductivity of carbonized and activated leather waste. Sustain. Chem. Pharm. 2023, 35, 101172. doi: 10.1016/j.scp.2023.101172
26. Ngwabebhoh FA; Bazi M.; Oladipo A. Adsorptive removal of multi-azo dye from aqueous phase using a semi-IPN superabsorbent chitosan-starch hydrogel. Chem. Eng. Res. Des. 2016, 112, 274–288. doi: 10.1016/j.cherd.2016.06.023
27. Chemical synthesis of highly electrically conductive polypyrrole. Synth. Met. 1989, 31, 311–318. doi: 10.1016/0379-6779(89)90798-4
28. Yang, XM; Zhu, ZX; Dai, TY; Lu, Y. Facile fabrication of functional polypyrrole nanotubes via a reactive self-degraded template. Macromol. Rapid Commun. 2005, 26, 1736–1740. doi: 10.1002/marc.200500514
29. Stejskal, J; Trchová, M. Conducting polypyrrole nanotubes: a review. Chem. Pap. 72, 1563–1595 (2018).
30. Stejskal, J; Prokeš J. Conductivity and morphology of polyaniline and polypyrrole prepared in the presence of organic dyes. Synth. Met. 2020, 264, 116373. doi: 10.1016/j.synthmet.2020.116373
31. Stejskal, J; Sapurina, I. Polyaniline: Thin films and colloidal dispersions (IUPAC technical report). Pure Appl. Chem. 2005, 77815–826. doi: 10.1351/pac200577050815
32. Beygisangchin, M; Rashid, SA; Shafie, S; Sadrolhosseini, AR; Lim, HN. Preparations, properties, and applications of polyaniline and polyaniline thin films – a review. Polymers 2021, 13, 2003. doi: 10.3390/polym13122003
33. Elyashevich, GK; Gerasimov, DI; Kuryndin, IS; Lavrentyev, VK; Rosova, EYu; Vylegzhanina, ME. Evolution of the surface structure and functional properties of the electroconducting polymer coatings onto porous films. Coatings 2022, 12, 51. doi: 10.3390/coatings12010051
34. Ngwabebhoh FA; Zandraa, O; Sáha, T; Stejskal, J; Trchová, M; Kopecký, D; Pfleger, J. Coating of leather with dye-containing antibacterial and conducting polypyrrole, Coatings 2023, 13, 608. doi: 10.3390/coatings13030608
35. Ćirić-Marjanović, G.; Pašti, I.; Mentus, S. One-dimensional nitrogen-containing carbon nanostructures. Prog. Mater. Sci. 2015, 69, 61–182. doi: 10.1016/j.pmatsci.2014.08.002
36. Souza Jr, FG; Michel, RC; Soares, BG. A methodology for studying the dependence of electrical resistivity with pressure in conducting composites. Polym. Test. 2005, 24, 998–1004. doi: 10.1016/j.polymertesting.2005.08.001.
37. Adetunji, OO; Chiou, NR; Epstein, AJ. Effect of pressure on the morphology of polyaniline nanostructures. Synth. Met. 2009, 159, 2263–2265. doi: 10.1016/j.synthmet. 2009.07.049
38. Stejskal, J; Trchová, M; Bober, P; Moravková, Z; Kopecký, D; Vrňata, M; Prokeš, J; Varga, M; Watzlová, E. Polypyrrole salts and bases: superior conductivity of nanotubes and their stability towards the loss of conductivity by deprotonation. RSC Adv. 2016, 6, 88382–88391. doi: 10.1039/c6ra19461c
39. Stejskal, J. Interaction of conducting polymers, polyaniline and polypyrrole, with organic dyes: polymer morphology control, dye adsorption and photocatalytic decomposition. Chem. Pap. 2020, 74, 1–54. doi: 10.1007/s11696-019-00982-9
40. Lyu, W; Li, JQ; Trchová, M; Wang, G; Liao, YZ; Bober, P; Stejskal, J. Fabrication of polyaniline/poly(vinyl alcohol)/montmorillonite hybrid aerogels toward efficient adsorption of organic dye pollutants. J. Hazard. Mater. 2022, 435, 129004. doi: 10.1016/j.jhazmat.2022.129004
41. Stejskal, J. Recent advances in the removal of organic dyes from aqueous media with conducting polymers, polyaniline and polypyrrole, and their composites. Polymers 2022, 14, 4243. doi: 10.3390/polym14194243

Preprints (www.preprints.org) | NOT PEER-REVIEWED | Posted: 13 September 2023 doi:10.20944/preprints202309.0810.v1

42. Porri, A; Baroncelli, R; Guglielminetti, L; Sarrocco, S; Guazzelli, L; Forti, M; Catelani, G; Valentini, G; Bazzichi, A; Franceschi, M; Vannacci, G. Fusarium oxysporum degradation and detoxification of a new textile-glycoconjugate azo dye (GAD). Fungal Biol. 2011, 115, 30–37. doi: 10.1016/j.funbio.2010.10.001
43. Jamal, M; Awadasseid, A; Su, XM. Exploring potential bacterial populations for enhanced anthraquinone dyes biodegradation: a critical review. Biotech. Lett. 2022, 44, 1011–1025. doi: 10.1007/s10529-022-03279-2
44. Liu, ML; Li, L; Sun, YX; Fu, ZJ; Cao, XL; Sun SP. Scalable conductive polymer membranes for ultrafast organic pollutants removal. J. Membr. Sci. 2020, 617, 118644. doi: 10.1016/j.memsci.2020.118644
45. Maldonado-Larios, L; Mayen-Mondragón, R; Martínez-Orozco, RD; Páramo-García, U; Gallardo-Rivas, MV; García-Alamilla, R. Electrochemically-assisted fabrication of titanium-dioxide/polyaniline nanocomposite films for the electroremediation of Congo red in aqueous effluents. Synth. Met. 2020, 268, 116464. doi: 10.1016/j.synthmet.2020.116464
46. Yu, HB; Che, M; Zhao, B; Lu, Y; Zhu, SY; Wang, XH; Qin, WC; Huo, MX. Enhanced electrosorption of rhodamine B over porous copper-nickel foam electrodes modified with graphene oxide/polypyrrole. Synth. Met. 2021, 262, 116332. doi: 10.1016/j.synthmet.2020.116332
47. Haque, MM; Wong, DKY. Improved dye entrapment-liberation performance at electrochemically synthesized polypyrrole-reduced graphene oxide nanocomposite films. J. Appl. Electrochem. 2017, 47, 777–788. doi: 10.1007/s10800-017-1079-9